MINERALOGICAL MAGAZINE, MARCH 1984, VOL. 48, PP. 85-91

Sulphide mineralogy of the Tomnadashan copper deposit and the Corrie Buie lead veins, south Loch Tayside, Scotland

R. A. D. PATTRICK

Department of Geology, University of Manchester, Manchester M13 9PL

ABSTRACT. Copper mineralization at Tomnadashan is associated with granitic lenses intruded into a small Caledonian diorite body. The mineralization occurs as disseminations and irregular veinlets and mainly comprises pyrite, chalcopyrite, tetrahedrite-tennantite, calcite, and quartz. There are small inclusions of bismuthinite, galena, aikinite [$(Cu,Pb,Fe,Bi)S_3$], and a mineral with a chemistry similar to hodrushite ($Cu_8Bi_{12}S_{22}$). The tetrahedrite contains up to 6.1 wt. % bismuth.

Four km to the south, at Corrie Buie, are quartz veins, hosted by meta-limestones, containing galena with minor amounts of chalcopyrite, pyrrhotite, sphalerite, electrum, schirmerite, and lillianite homologues.

The mineralogy of both deposits is consistent with that associated with acid magmatism. There are mineralogical similarities between the two deposits but the style of mineralization at Tomnadashan suggests a limited hydrothermal system and therefore the Corrie Buie veins may be related to felsic intrusives to the south.

AT Tomnadashan on the southern shore of Loch Tay (fig. 1) a small amount of copper mineralization occurs in a late Caledonian diorite intrusion. Four km to the south at Corrie Buie are quartz veins containing galena (fig. 1). Both deposits were mined on a small scale in the 19th century. The Tomnadashan mineralization is associated with granodiorite and granitic lenses within the diorite, the richest mineralization occurring close to the granodiorite–diorite contact and close to fractures associated with the lenses (Zabala, 1970; Halliday, 1961).

The Corrie Buie mineralization consists of a stockwork occurring in a small circular outcrop of nearly horizontal meta-limestones and calc-schists on the summit of Meall nan Oighreag (fig. 1). Thost (1860) reported three barren veins of east–west trend and eighteen parallel veins trending north–south composed of quartz and argentiferous galena (600 oz Ag/ton lead ore). The veins are entirely barren below the calcareous horizons, where they are hosted by hornblende schists and the quartz-rich 'Pitlochry' mica schists. These schists are part of the Upper Dalradian sequence situated within the inverted, flat-lying upper limb of the Tay Nappe.

The mineralogies of the Tomnadashan and Corrie Buie deposits were studied to investigate any possible genetic relationships between them, and also for comparison with the Tyndrum lead and zinc veins 30 km to the west (Pattrick, 1981). This entailed a detailed study of the sulphide minerals, the results of which are reported here.

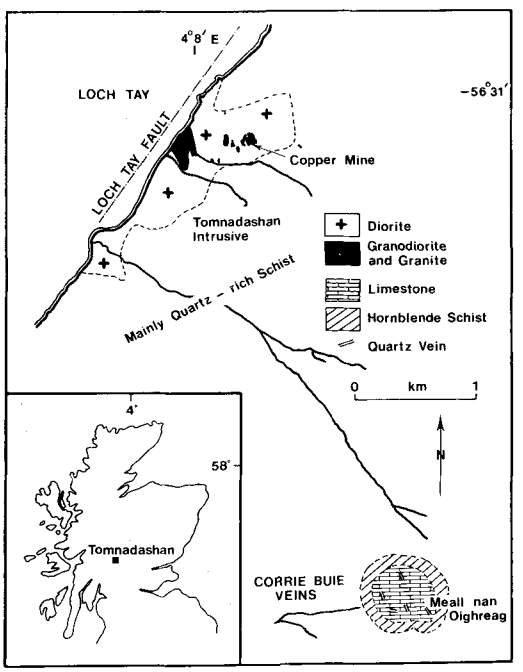

FIG. 1. The Tomnadashan mineralized intrusive and the Corrie Buie veins (including data from Zabala, 1970, and Geological Survey of Scotland 1″ series, Sheet 45).

Electron probe microanalysis

The electron probe microanalyses were carried out with instruments employing crystal spectrometers. The instruments used were a Microscan 5 at the Grant Institute of Geology, Edinburgh, and a Cameca Camebax at the Department of Geology, University of Manchester. The standards were: Cu, Ag, Fe, Zn, Au, Ni, Cd, HgS, FeS_2, GaSb, GaAs, ZnS, Bi_2S_3, and PbS. Many of the phases analysed were small inclusions, and great care was taken to ensure that the analyses were of homogeneous phases.

The Tomnadashan deposit

Pyrite, chalcopyrite, tetrahedrite, and molybdenite have been reported from the Tomnadashan mine along with the gangue minerals calcite, quartz, siderite, and minor baryte (Wilson and Cadell, 1884). The mineralization remaining at the mine contains high concentrations of pyrite (70% by volume in hand specimen) both as disseminations through the host rocks and concentrated along small irregular fractures. Chalcopyrite occurs with the pyrite, often as irregular masses up to 2 cm across. Tetrahedrite forms fine disseminations and occupies small fractures in the igneous host rock. Veins of calcite 2–10 cm wide contain pyrite, chalcopyrite, and tetrahedrite grains up to 2 cm across. Molybdenite was observed in calcite veinlets in the granite.

Examination of polished sections reveals the pyrite to be sub-idiomorphic cubic aggregates, often containing 30 μm blebs and small (< 20 μm wide) veinlets of chalcopyrite. The pyrite is usually slightly brecciated and sometimes replaced by chalcopyrite. Tetrahedrite is commonly associated with the chalcopyrite. Molybdenite is quite abundant in samples rich in pyrite, existing as 50–200 μm grains and often as platy aggregates of hexagonal crystals disseminated through the pyrite. Small fractures (20–40 μm) within the pyrite occasionally contain a varied mineralogy comprising chalcopyrite, galena, tetrahedrite, and native bismuth. The pyrite also contains small (~ 10 μm) blebs of bismuth-rich phases which were analysed by the electron probe as detailed below.

Electron probe analyses of tetrahedrite from Tomnadashan are given in Table I. The general formula of the tetrahedrite–tennantite series is $(Cu,Ag)^{1+}_{10}(Zn,Fe)^{2+}_{2}(Sb,As)^{3+}_{4}S_{13}$; significant concentrations of Hg, Cd, Pb, Bi, and Te have also been recorded. The analyses of the large grains in the calcite veins (analyses TOM 1 to 16, Table I) form two groups, a group of Sb-rich tetrahedrites and a group of As-rich tennantites. Most of the grains were found to be homogeneous and either As or Sb-rich but some consist of both types and detailed examination of these revealed an irregular-shaped compositional boundary running across the grains. The shape of the boundary and evidence from the replacement of pyrite at grain margins show the As-rich tennantites to have precipitated first.

The tetrahedrite–tennantite grains forming as blebs and inclusions within the pyrite (analyses TOM 17 and 18) are As-rich, whereas the tetrahedrite–tennantite grains occupying fractures (analyses TOM 19 to 21) are Sb-rich. These latter tetrahedrites also contain a significant amount of Bi. Bismuth is rarely found in tetrahedrite–tennantites, being first recorded by Boldyreva and Borodayer (1973) and subsequently by Oen and Kiefe (1976). In these published cases, the tetrahedrite is also associated with other Bi phases, indicating that high Bi concentrations in the mineralizing fluids allow the relatively large and electropositive Bi atom to compete with Sb and As for the trivalent site.

The divalent site in the tetrahedrite–tennantites is shared by Zn and Fe (Table I). However, analyses from grains of the mineral replacing pyrite (analyses TOM 4, 12, and 13) and occurring as inclusions in the pyrite (analyses TOM 17 and 18) show higher Fe, with $(Fe + Zn) > 2.0$. Non-stoichiometry in Fe-rich tetrahedrites has been previously recorded (Charlat and Levy, 1974; Pattrick, 1981) and, as there is no evidence of inclusions in the tetrahedrite–tennantites analysed, the excess Fe appears to have been inherited from the replaced pyrite. The analyses indicate this Fe to be replacing Cu^+, although this would cause a charge imbalance. Some of the extra Fe may be accommodated in voids in the tetrahedrite structure.

Electron probe analyses of the phases in fractures in pyrite confirm the presence of native bismuth, galena, and chalcopyrite. Some of the small blebs in the pyrite proved to be bismuthinite (Bi_2S_3). However, other blebs have a more complex chemistry (analyses TOM 22 to 28) and the analyses in Table II represent a Cu–Bi sulphosalt containing some Ag (presumably substituting for Cu) and a small amount of Fe and Pb. Kodera *et al.* (1970) describe a mineral hodrushite with a composition $Cu_{8.12}Bi_{11.54}Fe_{0.29}S_{22}$ and a suggested structural formula of $Cu_8Bi_{10}Me_2S_{22}$ where *Me* is a metal in octahedral co-ordination, often being Bi although Fe and Pb were both detected in their analyses. The analyses of material from Tomnadashan may therefore represent a variety of hodrushite with more extensive Fe and Pb substitution. The analyses (Table II) show Cu and Bi to be less than their 'ideal' concentrations ($Cu_8Bi_{12}S_{22}$). This indicates some Fe^{2+} and Pb^{2+} substitution for Cu^{2+} in the structure (see Kupcik and Makovicky, 1968) and occupancy of the Me_2 site by Pb^{VI} and Fe.

Table I Electron probe analyses of tetrahedrite-tennantites from Tomnadashan (wt %)

	Cu	Ag	Au	Ni	Zn	Fe	Cd	Hg	Sb	As	Bi	S	Total
TOM 1	38.77	0.53	0.00	0.03	5.71	2.03	0.08	0.69	22.91	3.91	0.35	25.37	100.38
TOM 2	42.36	0.09	0.25	0.05	4.28	3.86	0.05	0.73	5.18	17.09	0.16	26.78	100.38
TOM 3	42.29	0.01	0.00	0.01	4.10	4.16	0.12	0.06	5.03	17.09	0.41	27.62	101.45
TOM 4	40.92	0.30	0.00	0.03	2.00	7.61	0.00	0.03	4.76	16.90	0.42	27.62	100.59
TOM 5	39.41	0.59	0.00	0.04	4.31	3.05	0.00	0.18	20.42	6.75	0.00	25.55	100.30
TOM 6	39.00	0.58	0.22	0.03	4.60	2.85	0.11	0.16	21.14	6.01	0.22	25.44	100.36
TOM 7	38.90	0.50	0.11	0.01	4.82	2.80	0.07	0.00	19.11	7.67	0.27	25.08	99.34
TOM 8	38.46	0.55	0.03	0.04	4.86	2.72	0.08	0.00	23.24	4.59	0.13	25.29	99.99
TOM 9	38.95	0.34	0.19	0.04	4.78	2.72	0.03	0.00	22.81	4.85	0.09	25.50	100.30
TOM 10	39.18	0.59	0.00	0.00	4.66	2.91	0.15	0.00	19.42	7.18	0.17	25.62	99.88
TOM 11	39.18	0.49	0.00	0.24	4.81	3.03	0.02	0.00	21.21	6.20	0.01	25.50	100.69
TOM 12	41.02	0.18	0.00	0.04	2.03	7.64	0.00	0.00	4.77	17.10	0.00	27.69	100.47
TOM 13	40.92	0.24	0.00	0.01	1.93	7.38	0.00	0.00	5.74	16.52	0.00	27.67	100.41
TOM 14	38.82	0.52	0.00	0.00	4.90	2.69	0.01	0.00	20.97	6.00	0.45	25.56	99.92
TOM 15	41.51	0.38	0.00	0.00	3.71	4.13	0.15	0.00	9.75	14.61	0.00	27.00	101.24
TOM 16	38.58	0.01	0.00	0.00	4.72	3.04	0.00	0.19	20.65	6.54	0.59	25.54	99.86
TOM 17	41.63	0.03	-	-	1.05	7.41	-	-	2.58	18.04	0.60	29.88	101.22
TOM 18	41.67	0.07	-	-	0.88	7.23	-	-	2.50	17.77	0.72	30.03	100.86
TOM 19	38.18	0.55	-	-	3.62	4.99	-	-	17.40	5.74	5.97	24.61	102.06
TOM 20	39.30	0.25	-	-	2.42	5.88	-	-	13.69	9.03	5.74	26.19	102.55
TOM 21	37.26	0.33	-	-	3.29	5.01	-	-	18.74	4.69	6.13	25.62	101.07

Analyses recalculated to tetrahedrite-tennantite formula with $Me^{+} + Me^{2+}_{6} = 12$

	Cu	Ag	Au	Ni	Zn	Fe	Cd	Hg	Sb	As	Bi	S
TOM 1	9.86	0.08	0.00	0.01	1.41	0.59	0.00	0.06	3.04	0.84	0.03	12.78
TOM 2	9.90	0.01	0.02	0.01	0.97	1.03	0.01	0.05	0.63	3.39	0.01	12.40
TOM 3	9.93	0.00	0.00	0.00	0.94	1.11	0.02	0.00	0.62	3.50	0.03	12.85
TOM 4	9.49	0.04	0.00	0.01	0.45	2.01	0.00	0.00	0.58	3.32	0.03	12.69
TOM 5	9.95	0.09	0.00	0.01	1.06	0.88	0.00	0.02	2.69	1.45	0.00	12.78
TOM 6	9.90	0.09	0.02	0.01	1.14	0.82	0.02	0.01	2.80	1.29	0.02	12.80
TOM 7	9.90	0.08	0.01	0.00	1.19	0.81	0.01	0.00	2.54	1.66	0.02	13.01
TOM 8	9.88	0.08	0.02	0.01	1.21	0.80	0.01	0.00	3.12	1.00	0.01	12.88
TOM 9	9.94	0.05	0.02	0.01	1.19	0.79	0.01	0.00	3.04	1.05	0.01	12.90
TOM 10	9.91	0.09	0.00	0.00	1.15	0.84	0.02	0.00	2.56	1.54	0.01	12.84
TOM 11	9.87	0.07	0.00	0.01	1.18	0.87	0.00	0.00	2.79	1.33	0.00	12.73
TOM 12	9.50	0.02	0.00	0.01	0.46	2.01	0.00	0.00	0.58	3.36	0.00	12.70
TOM 13	9.56	0.03	0.00	0.00	0.44	1.96	0.00	0.00	0.70	3.28	0.00	12.82
TOM 14	9.92	0.08	0.00	0.00	1.22	0.78	0.00	0.00	2.80	1.30	0.04	12.94
TOM 15	9.94	0.05	0.00	0.01	0.86	1.13	0.02	0.00	1.22	2.97	0.00	12.80
TOM 16	9.92	0.00	0.00	0.00	1.18	0.89	0.00	0.02	2.77	1.43	0.05	13.01
TOM 17	9.78	0.00	-	-	0.24	1.98	-	-	0.32	3.59	0.04	13.91
TOM 18	9.85	0.01	-	-	0.20	1.94	-	-	0.31	3.56	0.05	14.02
TOM 19	9.61	0.08	-	-	0.89	1.43	-	-	2.28	1.23	0.46	12.77
TOM 20	9.27	0.04	-	-	0.58	1.66	-	-	1.77	1.90	0.44	12.84
TOM 21	9.65	0.05	-	-	0.83	1.48	-	-	2.53	1.03	0.48	13.14

There are, however, problems associated with simply ascribing the analyses in Table II to the mineral hodrushite. In studies of the Cu–Fe–Bi–S system, Sugaki and Shima (1978) report a phase of composition $Cu_{8.4}Fe_{1.2}Bi_{10.8}S_{22}$ (fig. 2) with a structure different to hodrushite. They also report, in synthetic studies of the Bi_2S_3–Cu_2S join at 450° and 500 °C, the existence of a phase D($Cu_{3+x}Bi_{5-x}S_9$) solid solution incorporating the compositions $Cu_3Bi_5S_9$ and $Cu_8Bi_{12}S_{22}$ (fig. 2). In the system Cu–Pb–Bi–S the phase D forms an extensive solid solution towards PbS at 450 °C (fig. 2) but its field reduces rapidly at lower temperatures. Buhlman (1971) found that $Cu_3Bi_5S_9$ was unstable below 435 ± 10 °C. Thus, work on synthetic systems reveals extensive substitution of Fe and Pb into compositions close to $Cu_8Bi_{12}S_{22}$ and $Cu_3Bi_5S_9$, and the analyses in Table II appear to represent a natural phase from the resulting solid-solution field.

Table II Electron probe analyses of Bi-rich inclusions in pyrite at Tomnadashan (wt. %)

	Cu	Ag	Pb	Fe	Bi	S	Total
TOM 22	8.67	4.05	3.18	1.23	63.10	19.17	99.40
TOM 23	10.87	3.96	0.95	1.19	64.35	19.31	100.63
TOM 24	9.87	4.00	2.02	1.93	64.43	19.22	101.47
TOM 25	10.10	3.03	4.06	1.06	62.33	19.22	99.80
TOM 26	10.63	3.41	4.72	1.80	60.61	19.36	100.53
TOM 27	9.98	5.56	5.03	2.03	61.02	19.07	100.69

Analyses recalculated to hodrushite formula* with S = 22

	Cu	Ag	Pb	Fe	Bi	S
TOM 22	5.02	1.38	0.57	0.81	11.11	22.00
TOM 23	6.25	1.34	0.17	0.78	11.25	22.00
TOM 24	5.07	1.36	0.36	1.27	11.32	22.00
TOM 25	5.83	1.03	0.72	0.70	10.95	22.00
TOM 26	6.10	1.15	0.83	1.17	10.57	22.00
TOM 27	5.81	1.22	0.90	1.35	10.80	22.00

*$Cu_8Bi_{12}S_{22}$

Analyses recalculated to $Cu_3Bi_5S_9$ with S = 9

	Cu	Ag	Pb	Fe	Bi	S
TOM 22	2.05	0.57	0.23	0.33	4.55	9.00
TOM 23	2.56	0.55	0.07	0.32	4.60	9.00
TOM 24	2.33	0.56	0.15	0.52	4.63	9.00
TOM 25	2.39	0.42	0.29	0.29	4.48	9.00
TOM 26	2.49	0.47	0.34	0.48	4.32	9.00
TOM 27	2.38	0.50	0.37	0.55	4.42	9.00

Analyses TOM 28 and 29 (Table III) came from small ($\sim$ 10 μm) grains in the pyrite and appear to be of the mineral aikinite, $CuPbBiS_3$, with some Fe substitution. The aikinite–bismuthinite series (fig. 2) contains six known phases (Harris and Chen, 1976). All reported aikinite analyses have Cu and Pb less than one in the structural formula (see Table III).

Textural evidence and the electron probe data reveal the paragenetic sequence to be pyrite + molybdenite + inclusions of bismuthinite, tennantite, aikinite, and possible hodrushite, followed by chalcopyrite + galena + native bismuth + tetrahedrite. The As–Sb zoning in the vein tetrahedrite-tennantites indicates either a stability gap in the series or a sudden change in physico-chemical conditions of ore formation. Bohmer (1964) did recognize a compositional gap in natural tetrahedrite–tennantites between 6 and 11 wt. % As (see Table I). This gap may, however, be due to different ore-forming environments favouring either As or Sb-rich solutions; intermediate compositions do in fact occur in nature and experimental studies show them to be stable. A change in the ore-forming condition may therefore explain the As–Sb zoning. Feiss (1974) noted in synthetic studies the rapid change from As-rich to Sb-rich members of the tetrahedrite–tennantite series in equilibrium with

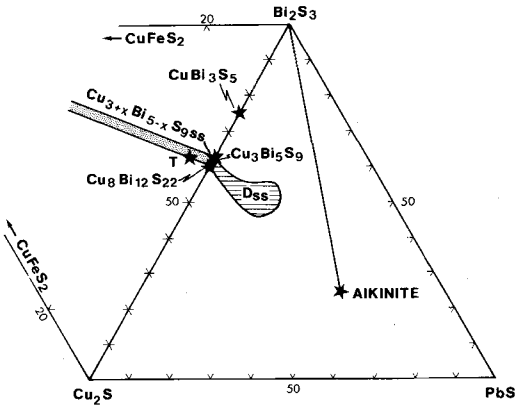

FIG. 2. Simplified representation of the Bi_2S_3–PbS–Cu_2S–$CuFeS_2$ system at 450 °C. E = emplectite; D_{ss} = extension of the $Cu_{3+x}Bi_{5-x}S_9$ solid solution towards PbS; T = $Cu_{8.4}Fe_{1.2}B_{10.8}S_{22}$ (data from Sugaki and Shima, 1978, and Harris and Chen, 1976).

enargite in response to a small drop in temperature in the range 500–390 °C and tetrahedrites are more common than tennantites in lower temperature sulphide ores. Thus the As–Sb compositional variation in the vein tetrahedrites may have been caused by a drop in the temperature of the mineralizing solutions.

Wallrock alteration. The alteration of the granodiorite in the main mineralized zone is intense. The feldspars are largely altered to sericite, though locally kaolinite, chlorite, and occasionally talc are the main alteration products. Calcite has been introduced, rutile is common, and sphene is also present. The rutile is closely associated with the ore minerals and sometimes it develops as needles along feldspar cleavages. Zabala (1970) recognized some propylitic alteration over the whole intrusion with chlorite–calcite–kaolinite alteration at the margins giving way to albite–kaolinite–calcite towards the centre.

TABLE III. *Electron probe analyses of aikinite from Tomnadashan (wt. %)*

	Cu	Ag	Pb	Fe	Bi	S	Total
TOM 28	10.29	0.00	32.56	2.26	36.90	17.02	99.03
TOM 29	9.81	0.00	34.18	1.61	36.62	17.19	99.41
Analyses recalculated to aikinite formula with S = 3							
TOM 28	0.92	0.00	0.89	0.23	1.00	3.00	
TOM 29	0.84	0.00	0.92	0.16	0.98	3.00	

The Corrie Buie veins

There is little evidence remaining of the reported extensive vein development. The limited amount of material left on the dumps at Corrie Buie comprises massive quartz containing galena cubes (up to 3 cm). Pyrrhotite was discovered in the present study and is associated with galena from one of the veins. Minor chalcopyrite, pyrite, and sphalerite were originally present and two 'small nuggets' of gold reported (Wilson and Cadell, 1884). Siderite and a late calcite stage of the mineralization were observed in dump samples.

Polished section study revealed the galena to be largely barren of inclusions, except for galena associated with the pyrrhotite. This galena contains bladed aggregates (up to 0.5 cm) of a strongly anisotropic mineral (blue grey) with a reflectance similar to galena. The same mineral occurs as individual small blades (~ 20 μm) in the galena in one or two orientations, indicating ex-solution along galena cleavages. Fractures in the galena (often associated with dolomite) contain native bismuth, pyrrhotite, electrum, grains of a mineral with the optical properties of schirmerite, and a single grain of emplectite. Irregular chalcopyrite grains (~ 200 μm) are also present.

Microprobe analyses of the bladed phases revealed these to be Pb–Bi–Ag sulphosalts (Table IV) and many of them appear to belong to the group of lillianite homologues, members of a structurally and chemically complex group which have been described in detail by Makovicky and Karup-Møller (1977*a*, *b*). Their crystal structure consists of layers of 'galena'-like structure joined by trigonally co-ordinated prisms (PbS_{6+2}). The layers are composed of chains of octahedra running diagonally across each layer. A lillianite homologue can be described by the number of octahedra (N) in the chain in each layer. Silver substitution into lillianite homologues is controlled by the relationship $2Pb \rightleftharpoons Bi + Ag$ and is limited by the sole occupancy of the trigonal-prismatic metal site by Pb. A line joining matildite ($AgBiS_2$) to galenobismutite ($PbBi_2S_4$) in fig. 3 represents the limit of Ag + Bi substitution. Lines drawn parallel to a line joining $AgBiS_2$ and PbS represent constant N values. Thus, the lillianite homologues form a number of series of constant N with Pb substitution by Ag + Bi. In nature the lillianite homologue compositions found are limited. The most populated series is the gustavite–lillianite line ($N = 4$) where analyses have been recorded for most of the range. Other phases within the series have been defined as separate mineral species such as treasurite, eskimoite, vikingite, ourayite, and heyrovskyite.

Table IV Electron probe analyses of Bi-rich inclusions in galena from Corrie Buie (wt. %)

	Ag	Bi	Pb	S	Total
A	7.63	55.67	18.00	17.25	98.55
B	7.96	54.15	18.45	16.84	97.40
C	7.21	53.98	20.82	17.36	99.38
D	14.00	51.04	16.16	16.76	99.95
E	8.88	49.81	25.06	16.31	100.05
F	7.18	47.88	28.42	16.60	100.07
G	9.42	47.68	25.93	16.70	99.73
H	6.57	47.65	29.11	16.51	99.83
J	7.15	47.48	26.71	16.70	98.03
K	6.31	47.29	29.19	16.21	99.32
L	6.55	44.64	30.48	16.42	98.09
M	5.73	43.28	37.51	14.99	101.50
N	6.67	41.74	36.16	15.96	100.53
P	5.74	40.42	35.76	16.36	98.27
Q	5.02	40.36	38.62	15.48	99.79
R	11.91	39.26	30.60	16.27	98.04
S	4.87	32.61	48.25	14.09	99.82
T	5.22	32.01	48.04	14.76	100.03
U	6.60	31.07	46.75	13.78	98.20
V	7.32	22.56	53.31	14.68	97.86
W	4.29	20.23	60.40	15.00	99.91
Y	22.18	52.48	6.82	17.29	99.77

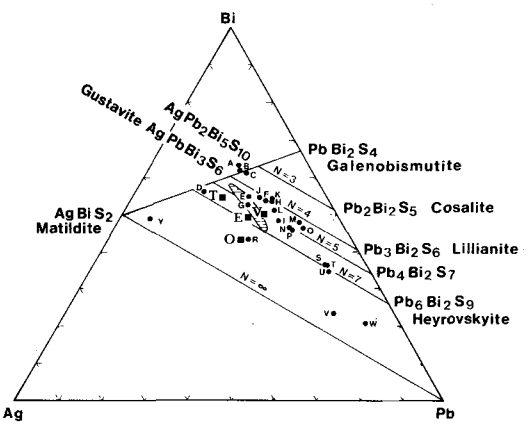

FIG. 3. The compositional plot Ag–Bi–Pb showing the compositions of the analysed inclusions in galena at Corrie Buie in relationship to the lillianite homologues (see text for explanation). T = treasurite; V = vikingite; O = ourayite; E = eskimoite; small letters A to Y denote analyses in this study and the shaded area is the composition field of schirmerite (adapted from Makovicky and Karup-Møller, 1977*a* and *b*).

The microprobe analyses from Corrie Buie are plotted on fig. 3. Four analyses, A–D, plot close to the fully substituted lillianite homologues with A–C close to $PbAgBi_3S_6$ (gustavite) with $N = 3.6$. Most analyses group between the gustavite–lillianite series line ($N = 4$) and the $Pb_4Si_2S_7$–$PbAg_2Bi_4S_6$ line ($N = 5$). This spread between constant-N series

could be the result of the phases containing components of $N = 4$ and $N = 5$ structures. Analyses S, T, and U plot on the $N = 7$ line and analysis R near to the composition of ourayite. Analyses E and G were of the inclusions with the optical properties of schirmerite and they plot in the known compositional field of that mineral. Analysis Y is close to the composition of matildite.

Analyses of the electrum inclusions revealed compositions varying between 65 and 36 wt. % Au. Analyses of the galena showed it to contain between 1.0 and 4.0 wt. % Bi, but less than 0.5 wt. % Ag, both these elements possibly being present in sub-microscopic inclusions.

The mineralogy of the Corrie Buie veins is typical of the vein ores which are associated with some acid intrusives. A similar assemblage is, for instance, found in the Darwin vein deposits, Southern California, where the mineralization is related to a quartz monzonite stock (Czamanske and Hall, 1975). The close proximity of the Corrie Buie veins to the mineralization at Tomnadashan (fig. 1) and their similar mineralogies suggest a genetic relationship.

Discussion

The mineralogy of the Corrie Buie veins was investigated partly for comparison with the Tyndrum lead and zinc veins (Pattrick, 1981), and there are significant differences. The breccia development prevalent in the Tyndrum veins is almost entirely absent at Corrie Buie. Mineralogical differences include the appearance of bismuth minerals and pyrrhotite, and the near absence of sphalerite and Sb-bearing phases. Pattrick (1981) suggests that there is no relationship between the Tyndrum veins and Caledonian magmatism and provides evidence for a Lower Carboniferous age for this mineralization. Stanley and Vaughan (1982), investigating the vein mineralization of the Lake District, distinguish between mineralization of Lower Devonian age related to Caledonian granites, with a mineralogy comprising pyrite + chalcopyrite + arsenopyrite + pyrrhotite + molybdenite and bismuth minerals, and veins of Lower Carboniferous age containing galena + sphalerite + baryte and antimony minerals. This distinction observed in the Lake District is the same as that between the late Caledonian Cu + Mo + As + Bi mineralization at Tomnadashan–Corrie Buie and the Lower Carboniferous Pb + Zn mineralization at Tyndrum.

The style of the mineralization, mineralogy, and associated alteration at Tomnadashan are similar to those observed in copper porphyries. The Caledonian calc-alkaline intrusives of Scotland are largely devoid of mineralization of this style despite their relationship to Silurian–early Devonian subduction (Philips *et al.*, 1976) and the high level of emplacement of the 'late' intrusions. However, a few of the smaller late intrusives have associated low-grade Cu + Mo mineralization, e.g. Kilmelford, Garbh Achadh, Ballachulish, Black Stockarton Moor, and Grudie (see Fortey, 1980). Plant *et al.* (1980) suggest that the copper porphyry style mineralization was in general limited because of the lack of available water in the medium- to high-grade metamorphic country rocks, the lack of major faults, and the continental landmass setting of the volcanic centres. They imply that the development of mineralization in some of these intrusives is due to their intrusion into relatively low-grade metamorphic rocks (e.g. Kilmelford and Ballachulish). However, even in these intrusives the mineralization is localized and of limited development with no evidence of a large-scale 'meteoric water' hydrothermal system. Harmon and Halliday (1980) using oxygen and strontium isotopes demonstrated that the late high-level Ben Cruachan granite had interacted extensively with O^{18}-depleted meteoric water, inferring its availability as a potential mineralizing fluid at the time of the intrusion of the 'late granites'.

The possibility thus arises that, although the mineralized intrusions are 'high level', they may not have reached the zone containing significant amounts of meteoric water. At Tomnadashan, the main mineralization was caused by a small but vigorous hydrothermal system centred on the later granitic member of the intrusion. It seems that the hydrothermal system could have been dominated by fluids expelled from the late fractionated volatile-rich magma intruded into the diorite. A rising andesitic magma generated from the mantle or basic lower crust normally contains between 1 and 5% H_2O (Gill, 1981). Burnham (1979) describes how, as this magma crystallizes at shallow levels, the volatile fraction (mainly water) can be exsolved and migrate towards the apex of the intrusion to be trapped by the crystalline outer shell of the intrusion. The magma associated with the volatile fraction will be more SiO_2-rich. Pressure within the apex of the intrusion builds up until hydraulic fracturing takes place (aided by resurgent boiling) leading to the release of the volatiles upward and resulting in mineralization of the top of the intrusion. Sometimes, the fractionated magma associated with the volatiles can also be intruded into the resultant fractures. Such a process would explain the close association of the mineralization and granitic lenses at Tomnadashan. The mineralization of the late Caledonian intrusives deserves further petrological, geochemical, and isotopic studies to investigate its genesis.

The Corrie Buie veins have a mineralogy consistent with vein mineralization associated with acid magmatism. However, if the Tomnadashan intrusive indeed had only a localized hydrothermal system, then the genesis of these lead veins may be related to another intrusion. The region contains felsite dykes, and 2 km to the SW is a large felsite intrusive that also deserves further investigation.

Acknowledgements. The author is indebted to Allan Hall and Michael Russell for critically reading the manuscript, to Peter Hill and David Plant for assistance with microprobe analysis, and to Philip Reagan for help with specimen collection. Part of the work was carried out at the University of Strathclyde and funded by an NERC studentship.

REFERENCES

Bohmer, H. (1964) *Geol. Soc. Am. Special Paper 82.*

Boldyreva, M. M., and Borodayer, Yu. S. (1973) *Dokl. Akad. Nauk. SSSR.* **R12,** 1424–5.

Buhlman, E. (1971) *Neues Jahrb. Mineral. Mh.* 137–41.

Burnham, D. W. (1979) In *The Geochemistry of Hydrothermal Ore Deposits*, 2nd edn. (H. L. Barnes, ed.). John Wiley and Sons, New York, 71–136.

Charlat, M., and Levy, C. (1974) *Bull. Soc. fr. Minéral. Crystallogr.* **97,** 241–50.

Czamanske, G. K., and Hall, W. E. (1975) *Econ. Geol.* **70,** 1092–110.

Feiss, P. G. (1974) Ibid. **69,** 383–90.

Fortey, N. J. (1980) *Trans. Inst. Mining Metall. B,* **80,** B173–6.

Gill, J. (1981) *Orogenic Andesites and Plate Tectonics.* Springer-Verlag.

Halliday, L. B. (1961) Loch Tay Copper. Geologist's report.

Harmon, R. S., and Halliday, A. N. (1980) *Nature,* **283,** 21–6.

Harris, D. C., and Chen, T. T. (1976) *Can. Mineral.* **14,** 194–205.

Kodera, M., Kupcik, V., and Makovicky, E. (1970) *Mineral. Mag.* **37,** 641–8.

Kupcik, V., and Makovicky, E. (1968) *Neues Jahrb. Mineral. Mh.* 236–7.

Makovicky, E., and Karup-Møller, S. (1977*a*) *Neues Jahrb. Mineral. Abh.* **131,** 187–207.

———(1977*b*) Ibid. 56–82.

Oen, I. S., and Kiefe, C. (1976) *Neues Jahrb. Mineral. Mh.* 94–6.

Pattrick, R. A. D. (1981) Ph.D. thesis, Univ. of Strathclyde (unpubl.).

Plant, J., Brown, G. C., Simpson, P. R., and Smith, R. T. (1980) *Trans. Inst. Mining Metall. B,* **89,** B198–210.

Philips, W. E. A., Stillman, C. J., and Murphy, T. (1976) *J. Geol. Soc. Lond.* **132,** 579–609.

Stanley, C. J., and Vaughan, D. J. (1982) Ibid. **139,** 569–79.

Sugaki, A., and Shima, H. (1978) *Experimental Petrology IV, Recent Progress of Natural Sciences in Japan,* **3,** 267–78.

Thost, C. H. G. (1860) *Proc. Geol. Soc.* 421–8.

Wilson, J. S. G., and Cadell, M. (1884) *R. Phys. Soc. Edinb.* **8,** 189–207.

Zabala, C. M. (1970) M.Sc. thesis, Univ. of Strathclyde (unpubl.).

[*Manuscript received 17 November 1982; revised 28 April 1983*]